


Article

PGC-1 α in melanoma: a key factor for antioxidant response and mitochondrial function[†]

Margalida Torrens-Mas^{1,2}, Daniel González-Hedström¹, Marta Abrisqueta³, Pilar Roca^{1,2}, Jordi Oliver^{1,2*} , Jorge Sastre-Serra^{1,2}

¹ Grupo Multidisciplinar de Oncología Traslacional, Institut Universitari d'Investigació en Ciències de la Salut (IUNICS), Palma, Illes Balears, Spain.

² Ciber Fisiopatología Obesidad y Nutrición (CB06/03) Instituto Salud Carlos III, Madrid, Spain.

Instituto de Investigación Sanitaria de Palma (IdISPa), Hospital Universitario Son Espases, edificio S. E-07120 Palma, Illes Balears, Spain.

³ Departamento de Bioquímica y Biología Molecular B e Inmunología, Universidad de Murcia e IMIB-Arrixaca. Campus de Ciencias de la Salud, El Palmar, Murcia.

*** Corresponding author:**

Dr. Jordi Oliver.

Departamento de Biología Fundamental y Ciencias de la Salud. Universitat de les Illes Balears. Cra de Valldemossa, km 7'5.07122 Palma de Mallorca, España.

Tel: (+34) 971259643

Fax: (+34) 971 173184

E-mail: jordi.oliver@uib.es

[†]This article has been accepted for publication and undergone full peer review but has not been through the copyediting, typesetting, pagination and proofreading process, which may lead to differences between this version and the Version of Record. Please cite this article as doi: [10.1002/jcb.26094]

Received 2 March 2017; Revised 8 April 2017; Accepted 25 April 2017

Journal of Cellular Biochemistry

This article is protected by copyright. All rights reserved

DOI 10.1002/jcb.26094

This article is protected by copyright. All rights reserved

Abstract

Melanocortin 1 receptor (MC1R) and BRAF are common mutations in melanoma. Through different pathways, they each regulate the expression of PGC-1 α , which is a key factor in the regulation of mitochondrial biogenesis and the antioxidant response. Our aim was to study the importance of the different regulatory characteristics of MC1R and BRAF on the pathways they regulate in melanoma. For this purpose, ROS production, levels of gene expression and enzymatic activities were analyzed in HBL and MeWo, with wild-type MC1R and BRAF, and A375 cells with mutant MC1R and BRAF. HBL cells showed a functional MC1R-PGC-1 α pathway and exhibited the lowest ROS production, probably because of a better mitochondrial pool and the presence of UCP2. On the other hand, MeWo cells showed elevated levels of PGC-1 α but also high ROS production, similar to the A375 cells, along with an activated antioxidant response and significantly low levels of UCP2. Finally, A375 cells are mutant for BRAF, and thus showed low levels of PGC-1 α . Consequently, A375 cells exhibited poor mitochondrial biogenesis and function, and no antioxidant response. These results show the importance of the activation of the MC1R-PGC-1 α pathway for mitochondrial biogenesis and function in melanoma development, as well as BRAF for the antioxidant response regulated by PGC-1 α . This article is protected by copyright. All rights reserved

Keywords: melanoma; oxidative stress; MC1R; BRAF; mitochondrial function.

1. Introduction

Cutaneous melanoma is one of the most severe forms of skin cancer and is the leading cause of death, with an incidence on the rise worldwide and expected to grow over the next few decades [1]. The main etiological factor for developing a melanoma is exposure to UV radiation [1,2], which in turn induces reactive oxygen species (ROS) production that leads to DNA damage and carcinogenesis [3,4].

A common mutation in melanoma is the constitutive activation of BRAF, which results in a reduced expression of MITF, a key regulator of melanogenesis, and PGC-1 α . BRAF-mutant melanomas show a metabolic shift towards a more glycolytic phenotype with a reduction in oxidative metabolism [5–7].

The human melanocortin 1 receptor (MC1R) expressed in epidermal melanocytes is also considered a gene for susceptibility to melanoma development, as it determines the skin phototype and UV radiation sensitivity [1,8]. Upon activation by the α -melanocyte stimulating hormone (α MSH), this receptor induces the synthesis of eumelanin [9–11], which is the main photoprotective physiological factor, as it can filter UV radiation, but it also protects against oxidative stress by acting as a ROS scavenger [1,2,12]. Loss of function of MC1R is associated to inefficient ROS detoxification, which can contribute to melanoma development [12].

Furthermore, recent studies suggest that MC1R also activates non-pigmentary pathways to stimulate the oxidative stress response, DNA repair and cell survival [8,12–14]. It has been described that activation of MC1R induces PGC-1 α (*Peroxisome proliferator-activated receptor gamma coactivator 1-alpha*) expression [5–7], which is the major regulator of mitochondrial biogenesis and antioxidant pathways [15,16]. PGC-1 α is usually up-regulated in cancer cells with elevated ROS levels and oxidative stress, and is associated to tumor development and aggressiveness, promoting cell proliferation and metastasis [17,18]. Moreover, recent studies suggest that increased PGC-1 α is implicated in the etiology and development of melanomas, which exert a high oxidative metabolism in order to maintain their growth and progression, and by protecting cells against apoptosis induction by ROS, thus allowing higher survival of cancer cells [5,19,20].

On the other hand, PGC-1 α has been described to participate in the response against oxidative stress with Foxo3a [21]. Foxo3a induces PGC-1 α expression and the two proteins interact with

each other to stimulate expression of antioxidant defenses, for both enzymatic ones such as superoxide dismutase (SOD), catalase, glutathione peroxidase (GPx), and non-enzymatic ones such as UCP2 [21–23].

The aim of this study was to analyze the importance of mitochondrial biogenesis and antioxidant response in melanoma. For this purpose, parameters such as ROS production, levels of gene expression and enzymatic activities were determined in three melanoma cell lines with different characteristics of MC1R and BRAF.

2. Materials and Methods

Reagents

Dulbecco's Modified Eagle's medium (DMEM) high glucose was purchased from GIBCO (Paisley, UK) and Eagle's Minimum Essential Medium (EMEM) from ATCC (Manassas, VA, USA). The synthetic analog of α -MSH, [Nle⁴,D-Phe⁷]- α -MSH or NDP-MSH was obtained from Tocris (Bristol, UK) and forskolin (FSK) from Sigma-Aldrich (St. Louis, MO, USA). Routine chemicals were supplied by Sigma-Aldrich (St. Louis, MO, USA), Roche (Barcelona, Spain), Panreac (Barcelona, Spain) and Bio-Rad Laboratories (Hercules, CA, USA).

Cell culture and treatments

Three different human melanoma cell lines, HBL (wild-type MC1R; wild-type BRAF), A375 (mutated MC1R; mutant BRAF) and MeWo (wild-type MC1R; wild-type BRAF) were used in all experiments. HBL and A375 cell lines were cultured in DMEM supplemented with 10% (v/v) heat-inactivated fetal bovine serum (FBS) and 1% (v/v) penicillin and streptomycin, while MeWo cells were maintained in EMEM medium with 10% FBS and 1% antibiotics. Cells were maintained in a humidified atmosphere of 5% CO₂ and 37 °C.

Cells were seeded in 100 mm culture plates for Western Blot and enzymatic activities analysis or in 96-well plates for cell viability and fluorometric assays. Cells were treated with 10⁻⁷ M NDP-MSH, a potent agonist at melanocortin receptors, for 48 hours. For PCR analysis, cells were plated in 6-well culture dishes and treated with 10⁻⁷ M NDP-MSH for 6 hours or 10⁻⁵ M FSK for 30 minutes. Finally, for those experiments analyzing UCP2 functionality, 50 μ M of genipin was added for 24 hours.

Cell viability assay

This article is protected by copyright. All rights reserved

Cells were treated as stated above. After treatment, cell viability was determined by crystal violet assay. Briefly, cells were stained with 0.5% (p/v) crystal violet in 30% (v/v) acetic acid for 10 min. After washing in distilled water, 100 μ l of methanol were added to solubilize the dye and absorbance was measured at 595 nm using a PowerWave XS Microplate Spectrophotometer (BioTek Instruments, Inc.).

Fluorometric measurement of ROS production and mitochondrial membrane potential

To measure ROS production, the Amplex[®] Red Hydrogen Peroxide/Peroxidase Assay Kit (Molecular Probes, Eugene, Oregon, USA) was used. Briefly, 50 μ M Amplex red reagent and 0.1 U/mL horseradish peroxidase were diluted in Krebs-Ringer phosphate buffer (145 mM NaCl, 4.86 mM KCl, 0.54 mM CaCl₂, 1.22 mM MgSO₄, 5.5 mM glucose, 5.7 mM sodium phosphate, pH 7.4) and the reaction mixture was added to cells. Fluorescence measurement was recorded at times 0, 15, 30 and 60 minutes. An FLx800 microplate fluorescence reader (Bio-Tek Winooski, Vermont, USA) was used, set at excitation and emission wavelengths of 571 and 585, respectively. Values were normalized per number of viable cells determined by crystal violet assay.

Mitochondrial membrane potential was analyzed by using tetramethylrhodamine methyl ester (TMRM), 100 nM. Cells were incubated with this probe for 15 minutes and fluorescence measurement was recorded with excitation and emission wavelengths set at of 552 and 576, respectively. Values were normalized per number of viable cells determined by crystal violet assay.

Real-time quantitative PCR

After treatment with NDP-MSH or FSK, total RNA was isolated from cultured cells using TriPure[®] isolation reagent (Roche, Barcelona, Spain) following the manufacturer's protocol and then quantified using a BioSpec-nano spectrophotometer (Shimadzu Biotech, Kyoto, Japan) set at 260 nm. For each sample, 1 μ g of the total RNA was reverse transcribed to cDNA at 42 °C for 60 min with 25 U MuLV reverse transcriptase in a 10 μ L volume of retrotranscription reaction mixture containing 10 mM Tris-HCl (pH 9.0), 50 mM KCl, 0.1% Triton X-100, 2.5 mM MgCl₂, 2.5 μ M random hexamers, 10 U RNase inhibitor, and 500 μ M each dNTP. Each cDNA was diluted 1/10 and aliquots were frozen (-20 °C) until the PCR reactions were carried out.

PCR was performed in triplicate samples using SYBR Green technology on a LightCycler 480 System II rapid thermal cycler (Roche Diagnostics, Basel, Switzerland). The genes, primers and
This article is protected by copyright. All rights reserved

temperatures for the annealing step are specified in Table 1. Total reaction volume was 10 μ L, containing 7.5 μ L Lightcycler® 480 SYBR Green I Master (containing 0.5 μ M of the sense and antisense specific primers) and 2.5 μ L of the cDNA template. The amplification program consisted of a preincubation step for denaturation of the template cDNA (5 min, 95 °C), followed by 45 cycles consisting of a denaturation step (10 s, 95 °C), an annealing step (10s, temperature depending on primers), and an elongation step (12s, 72 °C min). A negative control lacking cDNA template was run in each assay.

The Ct values of the real-time PCR were analyzed, taking into account the efficiency of the reaction and referring these results to the total DNA amount, using the GenEx Standard Software (Multi-DAnalises, Sweden).

Laser scanning confocal microscopy

Cells were plated and co-loaded with probes as described previously by Rodríguez-Enriquez et al. [24] with slight modifications. Cells were loaded with Mitotracker Green (MTG, 0.5 μ M) for 60 min at 37°C in complete culture medium. For the last 20 min of staining, LysoTracker Red (LTR, 0.5 μ M) was added under the same conditions. Finally, the last 5 min cells were incubated with 1 μ g propidium iodide (PI). The fluorescence of MTG, LTR and PI was monitored with a Leica Confocal microscope using 63x oil 14 N.A. objective lens. Excitation of probes and fluorescence emission were measured as in Rodríguez-Enriquez et al. [24].

Enzymatic activities

Cells were harvested 48h after NDP-MSH treatment by scraping them into 200 μ L of STE buffer (250 mM sucrose, 3.59 mM Trizma-Base, 16.4 Tris-HCl pH 7.4, 2mM EDTA, 40 mM KCl). Then, cells were disrupted by sonication at 40% amplitude for 10 seconds three times (VibraCell 75185) and centrifuged at 600xg for 10 min at 4 °C to remove cell debris. Protein content (supernatant) was determined with a bicinchoninic acid (BCA) protein assay kit (Pierce, Bonn, Germany) and the enzymatic assays were performed immediately after.

Cytochrome c oxidase (COX, Complex IV, EC 1.9.3.1) activity was measured using a spectrophotometric assay. Briefly, cell lysate was incubated in 0.1 M NaPO₄H₂, pH 7.0 in the presence of 2 μ g/mL catalase and 5 mM substrate DAB (3,3'-diaminebenzidine-tetrachloride) and then 100 μ M of reduced cytochrome c was added to start the reaction. The absorbance increment was followed for 25 min at 450 nm and 37°C. The generated slope is directly proportional to the activity of COX.

This article is protected by copyright. All rights reserved

ATP synthase (ATPase, ATP phosphohydrolase, Complex V, EC 3.6.1.3) activity was measured by following the oxidation of NADH at 340 nm and 37 °C. Briefly, cell lysate was incubated in assay buffer (0.33 M sucrose, 6.3 mM MgSO₄, 63.66 mM HEPES, 0.442 mM NADH, pH 8.0) in the presence of 2.5 mM Phospho(enol)pyruvic acid, 0.5 µg/mL Pyruvate Kinase, 0.25 µg/mL L-Lactic Dehydrogenase and 0.1 µg/mL antimycin. Then, 5 mM ATP was added to start the reaction. The absorbance reduction was followed for 15 min and the maximum slope was taken to analyze activity data. The generated slope is inversely proportional to the activity of ATPase.

Catalase (CAT, EC 1.11.1.6) activity was measured as described by Goth [25] and Hadwan & Abed [26] with few modifications. Briefly, cell lysate was incubated in assay buffer (100 mM K₂HPO₄/ KH₂PO₄, pH 7.0) and 65 mM hydrogen peroxide at 37 °C for 60 s. To stop the reaction, 32.4 mM ammonium molybdate ((NH₄)₆ Mo₇O₂₄ · 4 H₂O) was added and absorbance at 374 nm was measured. The higher the absorbance, the lower CAT activity.

Glutathione peroxidase (GPx, EC 1.11.1.9) activity was monitored by following the oxidation of NADPH by glutathione reductase coupled reaction. Cell lysates were incubated with assay buffer (50 mM Tris-HCl, 5 mM EDTA, pH 7.6), 35 mM reduced glutathione, 7.7 mM NADPH and 14 U/mL glutathione reductase. Reaction was started at 3 mM tert-butyl-hydroperoxide and monitored at 340 nm and 37 °C for 20 minutes. The generated slope is inversely proportional to the activity of GPx.

Glutathione reductase (GRd, EC 1.6.4.2) activity was measured by following the oxidation of NADPH at 340 nm and 37 °C. Briefly, cell lysates were incubated with assay buffer (50 mM phosphate buffer, 1 mM EDTA, pH 7.6) and 1.4 mM NADPH. To start reaction 3.5 oxidized glutathione was added to the mixture. The generated slope is inversely proportional to the activity of Grd.

Lactate dehydrogenase (LDH, EC 1.1.1.27) activity was measured by following the oxidation of NADH at 340 nm and 37 °C. Cell lysates were incubated with 80 mM Tris-HCl, 200 mM NaCl and 0.25 mM NADH. Reaction was started by adding 11 mM sodium pyruvate. The generated slope is directly proportional to the activity of LDH.

Total superoxide dismutase (SOD, EC 1.15.1.1) activity was determined by following the reduction of cytochrome c by measuring the absorbance at 550 nm, as described by Quick et al

(2000). MnSOD activity was measured the same way, adding 1 mM KCN in the reaction mixture.

Finally, Thioredoxin reductase (TrxR, 1.8.1.9) activity was determined by the reduction of DTNB (5,5'-dithiobis-2-nitrobenzoic acid) in the presence of NADPH, which generates a yellow compound measurable at 412 nm. To take into account any unspecific DTNB reduction, aurothiomalate was added to the reaction to inhibit TrxR.

cAMP assays

HBL and MeWo cells were plated in a 12-well dish, serum-deprived for 3 h and incubated with 10^{-7} M NDP-MSH or 10^{-5} M FSK for 30 min. Cells were quickly washed with 800 μ L ice-cold PBS and then lysed with 200 μ L 0.1 N HCl (preheated at 70°C) per well and scraped. The mix was freeze-dried, washed with 100 μ L H₂O and freeze-dried again twice. cAMP levels were measured by a commercial ELISA immunoassay (R&D Systems), following manufacturer's instructions. Briefly, samples and standards, a known concentration of cAMP-peroxidase conjugate, and a sheep antibody to cAMP were added into the wells of a microtiter plate coated with an antibody to capture sheep IgG. Following several washes, the substrate was added, which reacts with the bound cAMP-peroxidase conjugate. After a short incubation, the reaction was stopped and the intensity of the generated color was detected at 450 nm in a BioTek™ ELx800™ microtiter plate reader (BioTek, Bedfordshire, UK). Parallel dishes were used for protein determination by BCA assay.

Statistical analysis

The Statistical Program for the Social Sciences software for Windows (SPSS, version 21.0; SPSS Inc, Chicago, IL) was used for all statistical analyses. Results are presented as mean values \pm standard error of the mean (SEM) from six independent experiments. Data are referenced to the A375 cell line control group. The effects of NDP-MSH or FSK were assessed using the Student's t-test. Statistical significance was set at $P < 0.05$.

3. Results

ROS production was determined in three melanoma cell lines under basal conditions and in response to MC1R stimulation with NDP-MSH. ROS production was around 35% higher in A375 and MeWo compared to HBL cells, as shown in Figure 1. Interestingly, NDP-MSH treatment

This article is protected by copyright. All rights reserved

lowered ROS production only in HBL cells, while MeWo cells only showed a slight tendency to do so. As expected, NDP-MSH had no effect on ROS production in A375 cells.

Since MC1R induces PGC-1 α expression, the master regulator of mitochondrial biogenesis, the main genes involved in this process were studied. As seen in Table 2, PGC-1 α gene expression was significantly higher in both HBL and MeWo cells, both of which are wild-type for the receptor. TFAM and NRF1 expression was higher in HBL cells, while COXIV, ATPase and SIRT1 expression was higher in MeWo cells. Furthermore, treatment with NDP-MSH increased levels of TFAM, NRF1, COXIV and SIRT1 mRNAs in HBL cells, and lowered mtSSB and ATPase expression. In MeWo cells, only mtSSB expression increased with NDP-MSH treatment, while mRNA levels of COXIV, ATPase and SIRT1 dropped.

Given the differential response to NDP-MSH treatment observed in HBL and MeWo cell lines, cells were incubated with FSK, a potent adenylyl cyclase activator, to further check the ability to activate the MC1R pathway. Figure 2 shows that PGC-1 α increased significantly in A375 and HBL, but not in MeWo cells. This result suggests that MeWo cells have a non-fully functional MC1R signaling pathway, which could be in agreement with the observation that this cell line has a mutant adenylyl cyclase [28]. To further check this hypothesis, we performed a cAMP assay under basal conditions and under NDP-MSH and FSK stimulation for 30 min in HBL cells (wild-type for the adenylyl cyclase) and in MeWo cells (mutant for the adenylyl cyclase). As expected, HBL showed a great increase in cAMP levels, which was higher for the FSK treatment. On the contrary, cAMP levels in MeWo cells were minimal, in the range of 0.001 and 0.01 pmol, as shown in Figure 3.

To check mitochondrial functionality, enzymatic activities of COXIV, ATPase and LDH were next determined, as shown in Figure 4. COXIV activity was higher in HBL cells, and was enhanced by NDP-MSH stimulation by 41%. HBL also showed 40% less activity of ATPase compared to A375, but similar LDH activity. On the other hand, MeWo cells showed low levels for both COXIV and ATPase activity, while LDH activity more than doubled compared to A375 and HBL cells, yet was reduced by 58% by the NDP-MSH treatment.

Figure 5 shows the confocal images of the three cell lines under basal conditions, labeled with Hoechst, MTG and LTR. MeWo cells showed high MTG fluorescence (mitochondria) and low levels of LTR fluorescence (lysosomes), while HBL showed more co-localization of MTG and LTR.

The levels of different antioxidant defenses were studied, including both ROS-induced proteins and antioxidant enzymes. As seen in Table 3, MeWo cells presented the highest expression levels for *nrf2*, *foxo3a*, *mn-sod*, *cuzn-sod*, *cat*, *gpx*, *prx3*, *prx5* and *trx1*, but remained unresponsive to NDP-MSH treatment, as did the A375 cells. However, HBL cells did lower the expression of some enzymes under NDP-MSH stimulation. Figure 6 shows the enzymatic activities for catalase, TrxR, GPx, GRd, total SOD and Mn-SOD. In general, MeWo cells had the highest levels of antioxidant activities, except for GRd, while HBL cells showed, by far, lower enzymatic activities. NDP-MSH treatment only enhanced significantly the total SOD and MnSOD activities and lowered TrxR activity in HBL cells.

Finally, Figure 7 shows UCP2 mRNA levels under basal conditions and after the NDP-MSH treatment. Surprisingly, UCP2 expression levels were significantly different among the three cell lines. UCP2 expression was really low in MeWo cells (40% less than A375 cells), while HBL showed high levels of expression (more than double than those of the A375 cells). Both HBL and MeWo had elevated levels of UCP2 after the NDP-MSH treatment, although MeWo cells continued to have the lowest expression compared to the other cell lines. Since UCP2 seems to be a distinguishing characteristic, cells were incubated with genipin to functionally inhibit UCP2 activity and determine its importance. As expected, genipin affected HBL cells the most, and increased ROS production by 44% and mitochondrial membrane potential by 36%. ROS production was also increased in A375 cells with addition of genipin, but no significant differences were observed in MeWo cells.

4. Discussion

In this study, we have used three different melanoma cell lines with different functionality of the MC1R-PGC-1 α pathway. First, A375 cell line presents a mutant MC1R, expressing a non-functional receptor as A375 cells remain unresponsive to NDP-MSH treatment, and a mutation for BRAF (V600E), which leads to the constitutive activation of the MAPK pathway [5]. On the contrary, the HBL cell line is wild-type for both MC1R and BRAF and shows a marked activation of the signaling pathway with the NDP-MSH or FSK treatment as seen in our results and described previously by others [29]. Finally, the MeWo cell line is wild-type for MC1R and BRAF, but is mutant for the adenylate cyclase, as described in the canSAR database [28]. According to this database, MeWo cells show mutations in the following genes: ADCY3, ADCY4, ADCY7, ADCY10, which are classified as missense mutations. Furthermore, we have shown here a poor response to NDP-MSH and FSK treatment, as well as a minimal

residual response of MeWo cells under stimulation with NDP-MSH and FSK, as seen with the cAMP assay.

This study shows the importance of the MC1R-PGC-1 α pathway in mitochondrial biogenesis and function, which serve as a possible strategy to maintain ROS levels at the appropriate levels for a proliferative and aggressive phenotype, as seen in HBL cell line. HBL showed a functional MC1R, as evidenced by the induction of several genes with NDP-MSH treatment, especially PGC-1 α . In general, HBL cells presented higher gene expression levels of TFAM and NRF-1, mitochondrial biogenesis-related genes [16], and the highest COXIV activity, the main complex which regulates mitochondrial oxidative phosphorylation [30]. Moreover, confocal images showed a great turnover of mitochondria, as indicated by the co-localization of MTG and LTR, which could be a mechanism of mitochondrial quality control [31]. On the other hand, UCP2 has the ability to limit ROS production through proton leak and is considered an important defense against oxidative stress, promoting cell survival [32]. We have shown here the importance of UCP2 for HBL cell line, since treatment with genipin affected both mitochondrial membrane potential and ROS production.

These characteristics could provide an advantage for HBL cells, since they rely on oxidative phosphorylation and mitochondrial function for growth and to protect themselves against oxidative damage, as explained by Vazquez *et al.* [19]. Furthermore, LeBleu *et al.* [18] suggested that high PGC-1 α levels could promote cancer cell migration and metastasis. Considering these results, HBL could exhibit an improved, more functional mitochondrial pool with an enhanced ability to migrate.

When the MC1R-PGC-1 α signaling pathway is not working properly, as seen in A375 and MeWo cells, there is an important rise in ROS production. In response to stimulation with NDP-MSH and FSK, MeWo cells showed a poor response, suggesting that this pathway is not fully functional, which was also indicated by the low levels of cAMP under stimulation. Expression of all genes dependant on adenylate cyclase activity, that is, related to mitochondrial biogenesis and function, was lower compared to HBL and some of them dropped after NDP-MSH treatment. MeWo cells also exhibited the lowest COXIV and ATPase activities but the highest LDH activity, which indicates a poor mitochondrial function and activation of the glycolytic pathway [33]. Furthermore, confocal images showed a great number of mitochondria, which is probably from an attempt to fusion themselves in response to cellular stress and mitochondria damage [31].

Nevertheless, MeWo cells showed an important induction of antioxidant enzymes and their enzymatic activities as well as a high FOXO3a expression, which presumably is a response to the high basal ROS production observed. Recently, it has been described that the induction of the antioxidant enzymes is dependant on the expression of both PGC-1 α and FOXO3a, and that FOXO3a itself is a direct transcriptional regulator of PGC-1 α [21]. Therefore, since we have shown here that MC1R pathway is not fully functional, the high levels of PGC-1 α that characterize MeWo cells could be due to the activity of FOXO3a as a response to high oxidative stress.

Finally, the A375 cell line presents a mutant MC1R which results in the expression of a loss-of-function receptor. A375 cells are also mutant for BRAF, which is one of the most common alterations in melanoma and is characterized by a constitutive activation of BRAF. The activation of the BRAF/MAPK signaling pathway leads to the suppression of PGC-1 α and a decrease in oxidative metabolism and mitochondrial function [5]. In agreement with this, A375 cells remained unresponsive, since PGC-1 α levels were low and not sufficient to induce a response against ROS production, as seen with the antioxidant enzymes in MeWo cells which are wild-type for BRAF.

In conclusion, our results suggest that activation of the MC1R pathway could be a risk factor for melanoma development, not only due to its involvement in skin pigmentation, but also in the regulation of mitochondrial biogenesis and function. Furthermore, once the tumor is initiated a higher expression of PGC-1 α by activation of the MC1R pathway could suppose an advantage for cancer cells against oxidative stress and damage. Finally, we show here that the presence of a mutant BRAF could prevent the activation of antioxidant enzymes, thus impairing the response against oxidative stress.

Acknowledgements

This work was supported by a grant from *Asociación Española Contra el Cáncer* AECC-BALEARES 2014, and Fondo de Investigaciones Sanitarias of Instituto de Salud Carlos III (PI12/01827 and PI14/01434) of the Spanish Government, cofinanced by FEDER-Unión Europea (“Una manera de hacer Europa”). M. Torrens-Mas was funded by an FPU grant of Ministerio de Educación, Cultura y Deporte of Spanish Government.

Conflict of interest disclosure

The authors report no conflicts of interest. The authors alone are responsible for the content and writing of the paper.

References

- [1] V. Nikolaou, A.J. Stratigos, Emerging trends in the epidemiology of melanoma, *Br. J. Dermatol.* 170 (2014) 11–19. doi:10.1111/bjd.12492.
- [2] F. Rouzaud, A.L. Kadekaro, Z.A. Abdel-Malek, V.J. Hearing, MC1R and the response of melanocytes to ultraviolet radiation, *Mutat. Res. - Fundam. Mol. Mech. Mutagen.* 571 (2005) 133–152. doi:10.1016/j.mrfmmm.2004.09.014.
- [3] G.-H. Jin, Y. Liu, S.-Z. Jin, X.-D. Liu, S.-Z. Liu, UVB induced oxidative stress in human keratinocytes and protective effect of antioxidant agents., *Radiat. Environ. Biophys.* 46 (2007) 61–68. doi:10.1007/s00411-007-0096-1.
- [4] X. Song, N. Mosby, J. Yang, A. Xu, Z. Abdel-Malek, A.L. Kadekaro, alpha-MSH activates immediate defense responses to UV-induced oxidative stress in human melanocytes, *Pigment Cell Melanoma Res.* 22 (2009) 809–818. doi:10.1111/j.1755-148X.2009.00615.x.
- [5] R. Haq, J. Shoag, P. Andreu-Perez, S. Yokoyama, H. Edelman, G.C. Rowe, D.T. Frederick, A.D. Hurley, A. Nellore, A.L. Kung, J.A. Wargo, J.S. Song, D.E. Fisher, Z. Arany, H.R. Widlund, Oncogenic BRAF regulates oxidative metabolism via PGC1 α and MITF, *Cancer Cell.* 23 (2013) 302–315. doi:10.1016/j.ccr.2013.02.003.
- [6] Z. Ronai, The masters talk: The PGC-1 α -MITF axis as a melanoma energizer, *Pigment Cell Melanoma Res.* 26 (2013) 294–295. doi:10.1111/pcmr.12090.
- [7] J. Shoag, R. Haq, M. Zhang, L. Liu, G.C. Rowe, N. Koulisis, C. Farrel, C.I. Amos, Q. Wei, J.E. Lee, J. Zhang, T.S. Kupper, A.A. Qureshi, R. Cui, J. Han, PGC-1 Coactivators Regulate MITF and the Tanning Response, 49 (2013) 145–157. doi:10.1016/j.molcel.2012.10.027.PGC-1.
- [8] A.L. Kadekaro, S. Leachman, R.J. Kavanagh, V. Swope, P. Cassidy, D. Supp, M. Sartor, S. Schwemberger, G. Babcock, K. Wakamatsu, S. Ito, A. Koshoffer, R.E. Boissy, P. Manga, R.A. Sturm, Z.A. Abdel-Malek, Melanocortin 1 receptor genotype: An important determinant of the damage response of melanocytes to ultraviolet radiation, *FASEB J.* 24 (2010) 3850–3860. doi:10.1096/fj.10-158485.
- [9] M.C. Scott, K. Wakamatsu, S. Ito, A.L. Kadekaro, N. Kobayashi, J. Groden, R. Kavanagh, T. Takakuwa, V. Virador, V.J. Hearing, Z. a Abdel-Malek, Human melanocortin 1 receptor variants, receptor function and melanocyte response to UV radiation., *J. Cell Sci.* 115 (2002) 2349–2355.
- [10] E. Matichard, P. Verpillat, R. Meziani, B. Gérard, V. Descamps, E. Legroux, M. Burnouf, G. Bertrand, F. Bouscarat, a Archimbaud, C. Picard, L. Ollivaud, N. Basset-Seguín, D. Kerob, G. Lanternier, C. Lebbe, B. Crickx, B. Grandchamp, N. Soufir, Melanocortin 1 receptor (MC1R) gene variants may increase the risk of melanoma in France independently of clinical risk factors and UV exposure., *J. Med. Genet.* 41 (2004) e13. doi:10.1136/jmg.2003.011536.
- [11] A.B. Pérez Oliva, L.P. Fernández, C. Detorre, C. Herráiz, J.A. Martínez-Escribano, J. Benítez, J.A. Lozano Teruel, J.C. García-Bornón, C. Jiménez-Cervantes, G. Ribas, Identification and functional analysis of novel variants of the human melanocortin 1 receptor found in melanoma patients, *Hum. Mutat.* 30 (2009) 811–822.

doi:10.1002/humu.20971.

- [12] A.L. Kadekaro, J. Chen, J. Yang, S. Chen, J. Jameson, V.B. Swope, T. Cheng, M. Kadakia, Z. Abdel-Malek, Alpha-melanocyte-stimulating hormone suppresses oxidative stress through a p53-mediated signaling pathway in human melanocytes., *Mol. Cancer Res.* 10 (2012) 778–86. doi:10.1158/1541-7786.MCR-11-0436.
- [13] R.A. Newton, D.W. Roberts, J.H. Leonard, R.A. Sturm, Human melanocytes expressing MC1R variant alleles show impaired activation of multiple signaling pathways, *Peptides*. 28 (2007) 2387–2396. doi:10.1016/j.peptides.2007.10.003.
- [14] A.L. Kadekaro, R. Kavanagh, H. Kanto, S. Terzieva, J. Hauser, N. Kobayashi, S. Schwemberger, J. Cornelius, G. Babcock, H.G. Shertzer, G. Scott, Z.A. Abdel-Malek, alpha-melanocortin and endothelin-1 activate antiapoptotic pathways and reduce DNA damage in human melanocytes, *Cancer Res.* 65 (2005) 4292–4299. doi:10.1158/0008-5472.CAN-04-4535.
- [15] Z. Wu, P. Puigserver, U. Andersson, C. Zhang, G. Adelmant, V. Mootha, A. Troy, S. Cinti, B. Lowell, R.C. Scarpulla, B.M. Spiegelman, Mechanisms controlling mitochondrial biogenesis and respiration through the thermogenic coactivator PGC-1, *Cell.* 98 (1999) 115–124. doi:10.1016/S0092-8674(00)80611-X.
- [16] R.C. Scarpulla, R.B. Vega, D.P. Kelly, Transcriptional Integration of Mitochondrial Biogenesis, *Trends Endocrinol Metab.* 23 (2012) 459–466. doi:10.1016/j.tem.2012.06.006.
- [17] M.L. Boland, A.H. Chourasia, K.F. Macleod, Mitochondrial Dysfunction in Cancer, *Front. Oncol.* 3 (2013) 1–28. doi:10.3389/fonc.2013.00292.
- [18] V.S. LeBleu, J.T. O’Connell, K.N. Gonzalez Herrera, H. Wikman, K. Pantel, M.C. Haigis, F.M. de Carvalho, A. Damascena, L.T. Domingos Chinen, R.M. Rocha, J.M. Asara, R. Kalluri, PGC-1 α mediates mitochondrial biogenesis and oxidative phosphorylation in cancer cells to promote metastasis., *Nat. Cell Biol.* 16 (2014). doi:10.1038/ncb3039.
- [19] F. Vazquez, J.H. Lim, H. Chim, K. Bhalla, G. Girnun, K. Pierce, C.B. Clish, S.R. Granter, H.R. Widlund, B.M. Spiegelman, P. Puigserver, PGC-1 α Expression Defines a Subset of Human Melanoma Tumors with Increased Mitochondrial Capacity and Resistance to Oxidative Stress, *Cancer Cell.* 23 (2013) 287–301. doi:10.1016/j.ccr.2012.11.020.
- [20] H.G. Hambricht, P. Meng, A.P. Kumar, R. Ghosh, Inhibition of PI3K / AKT / mTOR axis disrupts oxidative stress- mediated survival of melanoma cells, *Oncotarget.* 6 (2015) 7195–7208.
- [21] Y. Olmos, I. Valle, S. Borniquel, A. Tierrez, E. Soria, S. Lamas, M. Monsalve, Mutual dependence of Foxo3a and PGC-1alpha in the induction of Oxidative stress genes, *J. Biol. Chem.* 284 (2009) 14476–14484. doi:10.1074/jbc.M807397200.
- [22] J. St-Pierre, S. Drori, M. Uldry, J.M. Silvaggi, J. Rhee, S. J?ger, C. Handschin, K. Zheng, J. Lin, W. Yang, D.K. Simon, R. Bachoo, B.M. Spiegelman, Suppression of Reactive Oxygen Species and Neurodegeneration by the PGC-1 Transcriptional Coactivators, *Cell.* 127 (2006) 397–408. doi:10.1016/j.cell.2006.09.024.
- [23] I. Valle, A. Álvarez-Barrientos, E. Arza, S. Lamas, M. Monsalve, PGC-1 α regulates the mitochondrial antioxidant defense system in vascular endothelial cells, *Cardiovasc. Res.*

66 (2005) 562–573. doi:10.1016/j.cardiores.2005.01.026.

- [24] S. Rodriguez-enriquez, Y. Kai, E. Maldonado, R.T. Currin, J.J. Lemasters, transition in remodeling of cultured rat hepatocytes, *5* (2014) 1099–1106.
- [25] L. Góth, A simple method for determination of serum catalase activity and revision of reference range., *Clin. Chim. Acta.* 196 (1991) 143–51.
- [26] M.H. Hadwan, H.N. Abed, Data supporting the spectrophotometric method for the estimation of catalase activity, *Data Br.* 6 (2016) 194–199. doi:10.1016/j.dib.2015.12.012.
- [27] D. Bogunovic, D.W.O.' Neill, I. Belitskaya-Levy, V. Vacic, Y.-L. Yu, S. Adams, F. Darvishian, R. Berman, R. Shapiro, A.C. Pavlick, S. Lonardi, J. Zavadil, I. Osman, N. Bhardwaj, A.J. Levine, Immune profile and mitotic index of metastatic melanoma lesions enhance clinical staging in predicting patient survival, *Proc. Natl. Acad. Sci. U. S. A.* 106 (2009) 20429–20434.
- [28] J.E. Tym, C. Mitsopoulos, E.A. Coker, P. Razaz, A.C. Schierz, A.A. Antolin, B. Al-Lazikani, canSAR: An updated cancer research and drug discovery knowledgebase, *Nucleic Acids Res.* 44 (2016) D938–D943. doi:10.1093/nar/gkv1030.
- [29] C. Herraiz, C. Jiménez-Cervantes, P. Zanna, J.C. García-Borrón, Melanocortin 1 receptor mutations impact differentially on signalling to the cAMP and the ERK mitogen-activated protein kinase pathways, *FEBS Lett.* 583 (2009) 3269–3274. doi:10.1016/j.febslet.2009.09.023.
- [30] Y. Li, J.S. Park, J.H. Deng, Y. Bai, Cytochrome c oxidase subunit IV is essential for assembly and respiratory function of the enzyme complex, *J. Bioenerg. Biomembr.* 38 (2006) 283–291. doi:10.1007/s10863-006-9052-z.
- [31] R. Youle, A. van der Bliek, Mitochondrial fission, fusion, and stress, *Science (80-.)*. 337 (2012) 1062–1065. doi:10.1126/science.1219855.Mitochondrial.
- [32] M.D. Brand, T.C. Esteves, Physiological functions of the mitochondrial uncoupling proteins UCP2 and UCP3, *Cell Metab.* 2 (2005) 85–93. doi:10.1016/j.cmet.2005.06.002.
- [33] M.G. Vander Heiden, L.C. Cantley, C.B. Thompson, P. Mammalian, C. Exhibit, A. Metabolism, Understanding the Warburg Effect : Cell Proliferation, *Science (80-.)*. 324 (2009) 1029–1034. doi:10.1126/science.1160809.

Figure legends

Figure 1. ROS production was significantly lower in HBL cells and was further reduced by NDP-MSH stimulation. ROS production was assessed fluorimetrically by Amplex Red® method after 48 h with 10^{-7} M NDP-MSH treatment. Values are expressed as means \pm SEM (n=6) and are referenced to A375 control group. Student's t test ($P < 0.05$) was performed to assess for significance. * indicates significant difference vs A375 control group; ° indicates significant difference between control-treated and NDP-MSH-treated cells; and # means significant difference vs HBL control group.

Figure 2. PGC-1 α mRNA levels increased after FSK treatment only in A375 and HBL cells. Levels of PGC-1 α expression were assessed by real-time PCR after 30 minutes of 10^{-5} M FSK (n=6). Student's t test ($P < 0.05$) was performed to assess for significance. * indicates significant difference between control-treated and FSK-treated cells.

Figure 3. cAMP levels after NDP-MSH and FSK stimulation. Levels of cAMP were determined in HBL and MeWo cells under basal conditions and after 30 min stimulation with NDP-MSH or FSK. The second graphic was represented with a more suitable scale bar to appreciate the difference. Student's t test ($P < 0.05$) was performed to assess for significance. * indicates significant difference between control-treated and treated cells.

Figure 4. HBL showed better mitochondrial function. Enzymatic activities of COX, ATPase and LDH were assessed spectrophotometrically as explained in the methods section (n=6). Student's t test ($P < 0.05$) was performed to assess for significance. * indicates significant difference vs A375 control group; ° indicates significant difference between control-treated and NDP-MSH-treated cells; and # means significant difference vs HBL control group.

Figure 5. HBL cells exhibited higher LTR fluorescence and MeWo showed higher MTG fluorescence. Confocal images were taken after loading cells with Mitotracker Green, LysoTracker Red and propidium iodide under basal conditions, as specified in the methods section. Scale bar: 25 μ m.

Figure 6. MeWo cells showed the highest activity for all antioxidant enzymes assessed. CAT, TrxR, total SOD, MnSOD, GPx and GRd activities were analyzed spectrophotometrically as explained in the methods section (n=6). CAT: catalase; TrxR: thioredoxin reductase; SOD: superoxide dismutase; MnSOD: manganese superoxide dismutase; GPx: glutathione peroxidase; GRd: glutathione reductase. Student's t test ($P < 0.05$) was performed to assess for significance. * indicates significant difference vs A375 control group; ° indicates significant difference between control-treated and NDP-MSH-treated cells; and # means significant difference vs HBL control group.

Figure 7. HBL cells showed the highest UCP2 expression and genipin treatment increased ROS production and mitochondrial membrane potential. UCP2 mRNA levels were assessed by real-time PCR after 10^{-7} NDP-MSH treatment. ROS production and mitochondrial membrane potential were assessed fluorimetrically by Amplex Red® and using the TMRM probe, respectively. These determinations were performed after treatment with 50 μ M genipin for 24

h. Student's t test ($P < 0.05$) was performed to assess for significance. * indicates significant difference between control- and treatment-treated cells.

Tables with captions

Table 1. Primers and conditions used for RT-PCR

gene	Forward Primer (5'-3') Reverse Primer (5'-3')	T° An. (°C)	gene	Forward Primer (5'-3') Reverse Primer (5'-3')	T° An. (°C)
<i>18s</i>	ggACACggACAggATTgACA ACCCACggAATCgAgAAAga	60	<i>mn-sod</i>	CgTgCTCCACACATCAATC TgAACgTCACgAggAgAAg	60
<i>pgc-1α</i>	TCAgTCCTCACTggTggACA TgCTTCgTCgTCAAAAACA	60	<i>cuzn-sod</i>	TCAggAgACCATTgCATCATT CgCTTTCCTgTCTTTgTACTTTCTTC	56
<i>tfam</i>	gTggTTTTCACTgTCTTggC ACTCCgCCCTATAAgCATCTTg	60	<i>cat</i>	CATCgCCACatgAATggATA CCAACtgggAtgAgAgggTA	60
<i>mtssb</i>	TgT gAA AAA ggg gTC TCg AA Tgg CCA Aag Aag AAT CAT CC	60	<i>gpx</i>	gCg gCg gCC Cag TCg gTg TA gAg CTT ggg gTC ggT CAT AA	60
<i>nrf1</i>	CCA CgT TAC Agg gAg gTg Ag TgT AgC TCC CTg CTg CAT CT	60	<i>grd</i>	TCACgCAGTTACCAAAAggAAA CACACCCAAGTCCCCTgCATAgT	64
<i>nrf2</i>	gCg Acg gAA AgA gTA TgA gC gTT ggC AgA TCC ACT ggT TT	60	<i>prx2</i>	CCAgACgCTTgTCTgAggAT ACgTTgggCTTAATCgTgTC	60
<i>coxiv</i>	AAC gAg Tgg AAg ACg gTT gT TCA TgT CCA gCA TCC TCT Tg	60	<i>prx3</i>	gCCgTTgTCATggAgAgTT TCCACTgAgACTgCgACAAC	53
<i>atpase</i>	CAT TgT ggA CgT TCC AgT Tg ATT ggC ACC AAg CTA TCC AC	55	<i>prx5</i>	ACggTgCAGTgAAggAgAgT CAggAACTCCAAACgCACA	60
<i>sirt1</i>	gCAGATTAgTAggCggCTTg TCTggCATgTCCCACATCA	54	<i>prx6</i>	CgTgTggTgTTTgTTTTTgg CCATCACACTATCCCACATCC	60
<i>sirt3</i>	CggCTACACgCAGAACATC CAGAggCTCCCCAAAgAACAC	56	<i>trx1</i>	CTgCTTTTCaggAAgCCTTg TgTTggCATgCATTTgACTT	60
<i>foxo3a</i>	gCA AgC ACA gAg TTg gAT gA CAG gTC gTC CAT gAg gTT TT	60	<i>trx2</i>	gCAAAATCCAAACCACggg CCCTAgAggAgggACCggAAg	60
<i>ucp2</i>	ggTggTTCggAgATACCAAg CTCgggCAATggTCTTgTtag	60	<i>trx2</i>	TCgAgTCCCAgACACCgAA TgATCgCTATgggTgTCAgC	60

T° An.: annealing temperature; *pgc-1α*: peroxisome proliferator-activated receptor gamma coactivator 1-alpha; *tfam*: mitochondrial transcription factor A; *mtssb*: mitochondrial single stranded DNA-binding protein; *nrf1*: nuclear respiratory factor 1; *nrf2*: nuclear respiratory factor 2; *coxiv*: cytochrome c oxidase subunit IV; *atpase*: ATPase/ATP synthase; *sirt1*: sirtuin 1; *sirt3*: sirtuin 3; *foxo3a*: forkhead box O3; *ucp2*: uncoupling protein 2; *mn-sod*: manganese superoxide dismutase; *cuzn-sod*: copper-zinc superoxide dismutase; *cat*: catalase; *gpx*: glutathione peroxidase; *grd*: glutathione reductase; *prx2*: peroxiredoxin 2; *prx3*: peroxiredoxin

3; prx5: peroxiredoxin 5; prx6: peroxiredoxin 6; trx1: thioredoxin 1; trx2: thioredoxin 2; trxr2: thioredoxin reductase.

Table 2. Mitochondrial biogenesis and function-related genes mRNA expression in A375, HBL and MeWo cell lines after NDP-MSH treatment

	A375		HBL		MeWo	
	Control	NDP-MSH	Control	NDP-MSH	Control	NDP-MSH
<i>pgc-1α</i>	1.00 ± 0.08	1.04 ± 0.13	9.35 ± 1.45	19.0 ± 1.73*	11.5 ± 0.73	13.9 ± 0.68*
<i>tfam</i>	1.00 ± 0.04	0.96 ± 0.06	1.97 ± 0.20	2.76 ± 0.38*	1.68 ± 0.17	1.53 ± 0.16
<i>mtssb</i>	1.00 ± 0.09	0.92 ± 0.09	0.89 ± 0.10	0.64 ± 0.09*	0.95 ± 0.12	1.61 ± 0.31*
<i>nrf1</i>	1.00 ± 0.07	0.95 ± 0.05	1.13 ± 0.09	1.66 ± 0.23*	0.76 ± 0.09	0.77 ± 0.09
<i>coxiv</i>	1.00 ± 0.09	1.02 ± 0.06	1.28 ± 0.05	1.56 ± 0.09*	2.35 ± 0.21	1.64 ± 0.08*
<i>atpase</i>	1.00 ± 0.16	1.04 ± 0.12	1.38 ± 0.10	0.96 ± 0.05*	1.47 ± 0.05	1.23 ± 0.12*
<i>sirt1</i>	1.00 ± 0.07	1.02 ± 0.08	1.74 ± 0.10	2.17 ± 0.19*	2.57 ± 0.22	1.96 ± 0.16*

Data represent the means ± SEM (n=9). Values of control (vehicle-treated) A375 were set at 1.00. *pgc-1α*: peroxisome proliferator-activated receptor gamma coactivator 1-alpha; *tfam*: mitochondrial transcription factor A; *mtssb*: mitochondrial single stranded DNA-binding protein; *nrf1*: nuclear respiratory factor 1; *coxiv*: cytochrome c oxidase subunit IV; *atpase*: ATPase/ATP synthase; *sirt1*: sirtuin 1.

* Significant difference between NDP-MSH-treated and vehicle-treated cell lines (Student's *t*-test; P<0.05).

Table 3. Antioxidant defenses-related genes mRNA expression in A375, HBL and MeWo cell lines after NDP-MSH treatment

	A375		HBL		MeWo	
	Control	NDP-MSH	Control	NDP-MSH	Control	NDP-MSH
<i>nrf2</i>	1.00 ± 0.04	0.97 ± 0.06	0.86 ± 0.05	0.79 ± 0.12	1.51 ± 0.20	1.67 ± 0.23
<i>sirt3</i>	1.00 ± 0.09	0.90 ± 0.09	1.07 ± 0.09	1.21 ± 0.08	1.19 ± 0.14	1.15 ± 0.27
<i>foxo3a</i>	1.00 ± 0.14	1.09 ± 0.06	1.68 ± 0.20	1.33 ± 0.01	1.99 ± 0.28	1.74 ± 0.19
<i>mn-sod</i>	1.00 ± 0.09	0.98 ± 0.14	0.92 ± 0.13	1.31 ± 0.18*	2.04 ± 0.26	1.93 ± 0.26
<i>cuzn-sod</i>	1.00 ± 0.08	1.04 ± 0.10	1.48 ± 0.18	1.87 ± 0.14	1.84 ± 0.34	1.91 ± 0.74
<i>cat</i>	1.00 ± 0.08	0.90 ± 0.08	1.90 ± 0.18	2.41 ± 0.25	3.13 ± 0.67	3.15 ± 0.78
<i>gpx</i>	1.00 ± 0.08	0.99 ± 0.09	0.89 ± 0.09	0.57 ± 0.04*	1.26 ± 0.14	1.03 ± 0.10
<i>grd</i>	1.00 ± 0.11	1.13 ± 0.12	1.09 ± 0.09	0.79 ± 0.04*	1.08 ± 0.10	0.88 ± 0.05
<i>prx2</i>	1.00 ± 0.13	0.99 ± 0.09	1.58 ± 0.33	1.03 ± 0.07	0.51 ± 0.02	0.44 ± 0.04
<i>prx3</i>	1.00 ± 0.10	0.96 ± 0.08	1.35 ± 0.12	1.25 ± 0.05	1.26 ± 0.11	1.36 ± 0.08
<i>prx5</i>	1.00 ± 0.18	1.07 ± 0.10	1.08 ± 0.16	0.67 ± 0.10*	2.08 ± 0.11	1.68 ± 0.07*
<i>prx6</i>	1.00 ± 0.14	0.93 ± 0.04	0.74 ± 0.11	0.54 ± 0.02	0.44 ± 0.04	0.41 ± 0.01
<i>trx1</i>	1.00 ± 0.06	1.04 ± 0.05	2.14 ± 0.16	1.54 ± 0.06*	1.93 ± 0.21	2.02 ± 0.07
<i>trx2</i>	1.00 ± 0.16	0.88 ± 0.10	1.33 ± 0.10	0.90 ± 0.08*	0.94 ± 0.31	0.47 ± 0.04
<i>trxr2</i>	1.00 ± 0.12	0.99 ± 0.14	4.52 ± 0.17	2.28 ± 0.35*	3.93 ± 0.28	2.77 ± 0.45

Data represent the means ± SEM (n=9). Values of control (vehicle-treated) A375 were set at 1.00. *nrf2*: nuclear respiratory factor 2; *sirt3*: sirtuin 3; *foxo3a*: forkhead box O3; *mn-sod*: manganese superoxide dismutase; *cuzn-sod*: copper-zinc superoxide dismutase; *cat*: catalase; *gpx*: glutathione peroxidase; *grd*: glutathione reductase; *prx2*: peroxiredoxin 2; *prx3*: peroxiredoxin 3; *prx5*: peroxiredoxin 5; *prx6*: peroxiredoxin 6; *trx1*: thioredoxin 1; *trx2*: thioredoxin 2; *trxr2*: thioredoxin reductase.

* Significant difference between NDP-MSH-treated and vehicle-treated cell lines (Student's *t*-test; P<0.05).

Figure 1

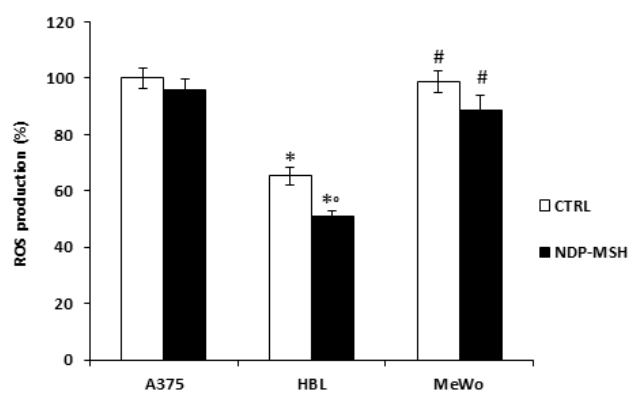


Figure 2

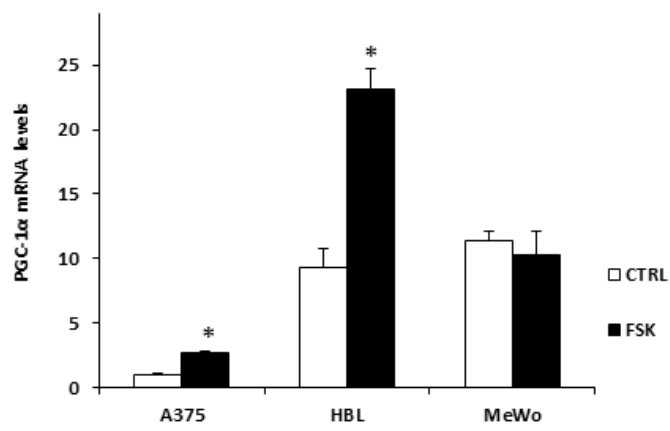


Figure 3

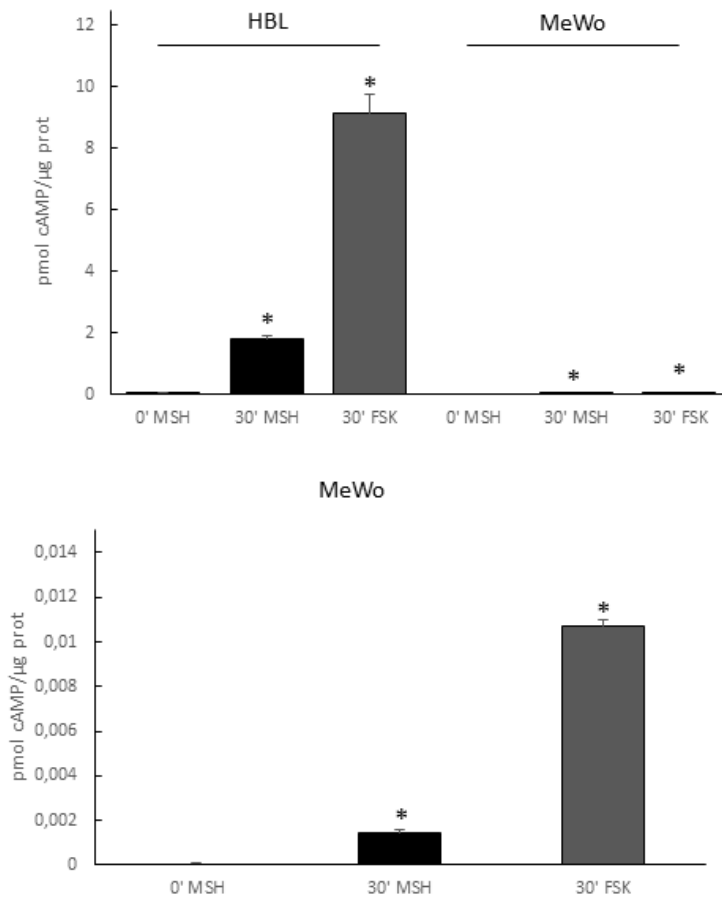


Figure4

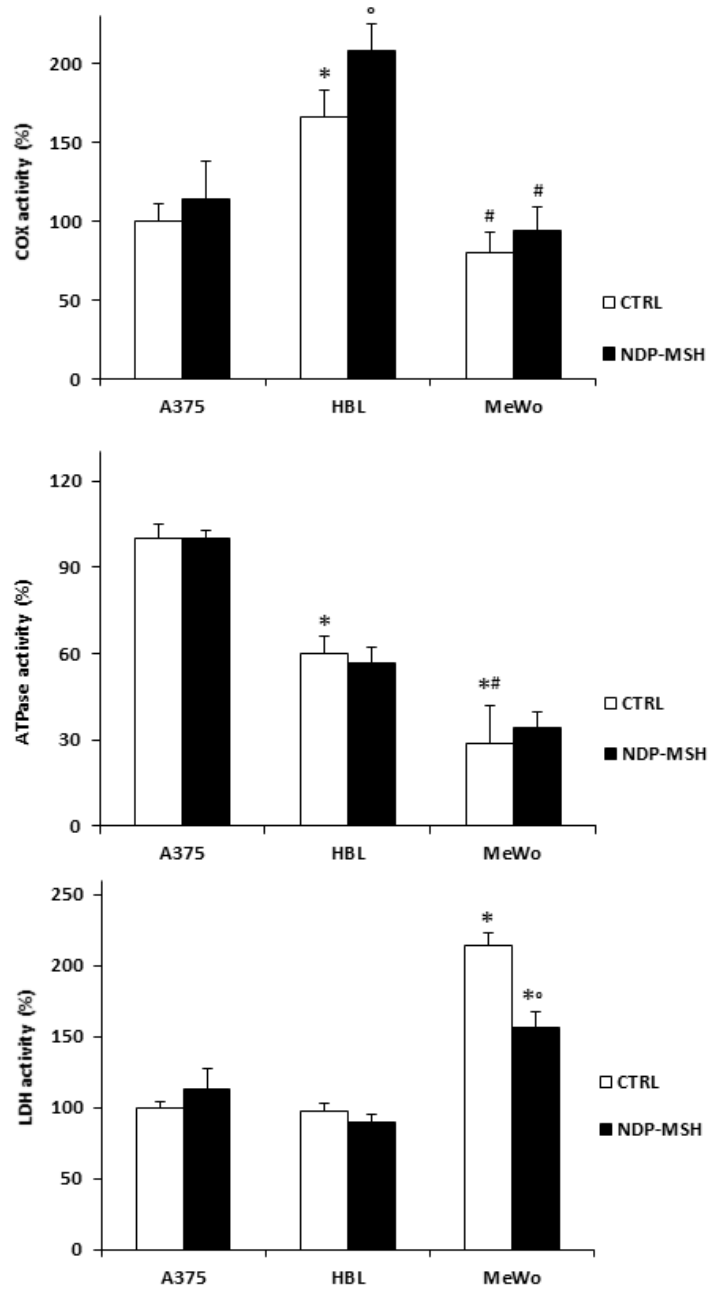
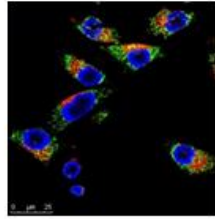
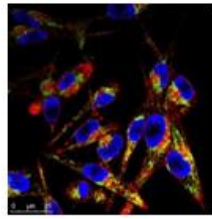


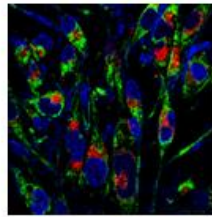
Figure5



A375



HBL



MeWo

Figure 6

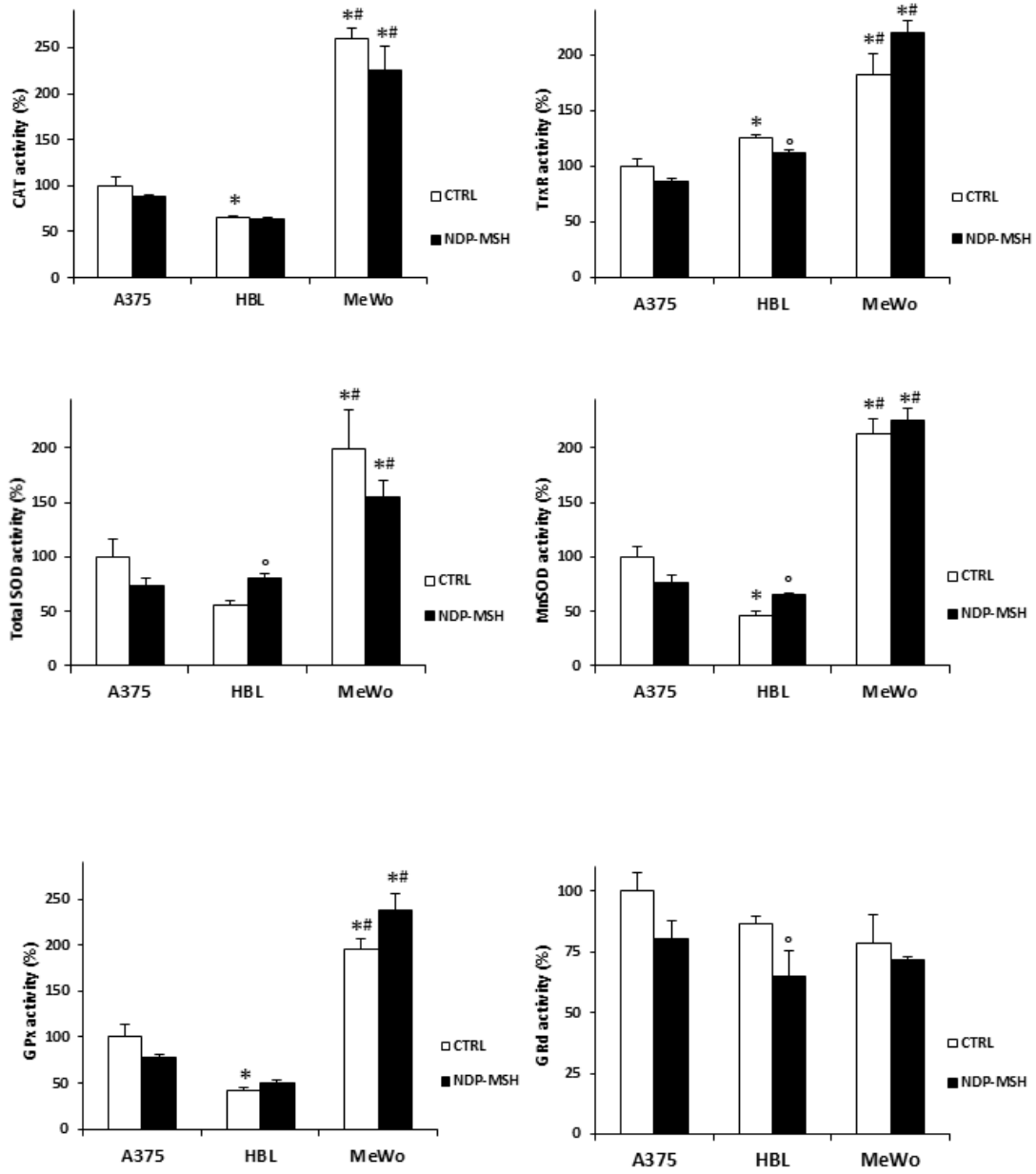


Figure 7

